

M. Dutt

Department of Materials Science and Metallurgy, University of Cambridge, Cambridge CB1 7XE, UK

B. Hancock

Pfizer Global Research and Development, Groton, CT 06340 USA

C. Bentham

Pfizer Global Research and Development, Sandwich, Kent CT13 9NJ, UK

J. Elliott

Department of Materials Science and Metallurgy, University of Cambridge, Cambridge CB1 7XE, UK

Pharmaceutical powder blends used to generate tablets are complex multicomponent mixtures of the drug powder and excipients which facilitate the delivery of the required drug. The individual constituents of these blends can be noncohesive and cohesive powders. We study the geometric and mechanical characteristics of idealized mixtures of excipient particle packings, for a small but representative number of dry noncohesive particles, generated via gravitational compaction followed by uniaxial compaction. We discuss particle packings in 2- and 3- component mixtures of microcrystalline cellulose (MCC) & lactose and MCC, starch & lactose, respectively. We have computed the evolution of the force and stress distributions in monodisperse and polydisperse mixtures comprised of equal parts of each excipient; comparisons are made with results for particles packings of pure blends of MCC and lactose. We also compute the stress-strain relations for these mixtures. In order to obtain insight into details of the particle packings, we calculate the coordination number, packing fraction, radial distribution functions and contact angle distributions for the various mixtures. The numerical experiments have been performed on spheroidal idealizations of the excipient grains using Discrete Element Method simulations (Dutt et al., 2004 submitted).

1 INTRODUCTION

Most industrial powder processes handle mixtures of powders whose components may vary in either, or both, material properties and size distributions. The pharmaceutical industry (Alderborn & Nystrom 1996) handles large volumes of powder blends which comprise of the excipients and the drug powder. A lot of the existing work in the area of granular materials (Jaeger, Nagel & Behringer 1996) has focused on the behavior of the agglomerates of particles with identical material properties (Silbert, Ertas, Grest, Halsey & Levine 2002)-(Makse, Gland, Johnson & Schwartz 2000). We address queries related to the geometric aspects of the packing structure and the material response to an externally applied strain, with emphasis on the load distribution, of these mixtures of materials with focus on mixtures of pharmaceutical excipients.

We have structured the paper into the following sections: section 2 provides a description of the two systems we have focused upon for this paper; section 3 describes the details of the the numerical model and the numerical experiment; section 4 presents the results from our numerical experiments and section 5 summarizes the proceedings.

2 MIXTURES OF PHARMACEUTICAL EXCIPIENTS

We are interested in studying the behavior of mixtures of common pharmaceutical excipients such as microcrystalline cellulose (MCC), lactose and starch. We consider mixtures of two and three excipients, and study their packing structure and material response to the applied strain. We focus our studies on two mixtures, both with a total of 1800 particles: sample S1 is a mixture of

equal parts of 200 μm diameter MCC and lactose spheres, and sample S2 is a mixture of equal parts of 200 μm diameter MCC, lactose and starch spheres. To understand the behavior of the mixtures of different materials, we have chosen to work with equal concentrations of monodisperse spheres, thereby excluding additional complications which might arise from differing concentrations, or size dispersity of the individual components.

3 THE NUMERICAL MODEL AND THE NUMERICAL EXPERIMENT

We have carried out our numerical experiments using 3D Discrete Element Method (DEM) simulations (Cundall & Strack 1979). We study spherical non-rigid particles which can suffer small deformations upon contact with the other particles. The only interaction forces of relevance to our system are the mechanical contact forces; therefore, the degree of deformation at a contact will determine the contact force experienced by the two particles forming the contact. We have used a slightly modified form of the Hertzian contact force law called the Hertz-Kuwabara-Kono contact force model to represent the normal contact interactions, and a linear damped harmonic oscillator model to represent the tangential contact interactions (Schafer, Dippel & Wolf 1996). The interparticle interaction model utilizes the particle material properties, such as the Young's modulus and the Poisson ratio, along with the contact deformations and the relative velocities at the contact surface to determine the contact forces (Schafer, Dippel & Wolf 1996). The Young's moduli for MCC, lactose and starch are 9.08×10^9 Pa, 3.21×10^9 Pa and 3.71×10^9 Pa, respectively; all three materials have a Poisson ratio equal to 0.3 (Alderborn & Nystrom 1996). Interparticle substrate friction has been accounted for by including the Coulomb's friction criteria (Aastrom, Herrmann & Timonen 2000), and thereby, adding two more control parameters: the coefficient of kinetic friction μ_k and the coefficient of static friction μ_{stat} . For ease of calculation, we have taken the coefficients of friction to have identical values ($\mu_k = \mu_{stat}$). All simulations are performed in two stages: the particles are allowed to settle under gravity followed by constant strain uniaxial compaction at 1 mm/s. Each phase occurs for a preset interval of time. We have used two-dimensional periodic boundary conditions in our simulations, and we have bounded the system by planes normal to the direction of gravity by surfaces comprised of agglomerates of particles of the same material as those in the bulk. Further details of the interparticle interactions and the numerical simulations can be found in (Dutt, Hancock, Bentham & Elliott 2005).

4 RESULTS

We have studied the mixtures by focusing on the geometric aspects of the packings and the response to the applied strain. We have characterized the geometric aspects of the packings generated by computing the packing fraction, coordination number, the radial distribution function and the distribution of contacts and the contact angles. The response to the applied strain has been studied by computing the normal and tangential contact force distributions. In each of the graphs, the first and second numbers are the values for μ_k and μ_{stat} , respectively.

Existing work (Clarke & Jonsson 1993) has found the mechanically stable packings of monodisperse spheres of a single material to have loose random packing (RLP) and close random packing (RCP) values of the packing fraction to approximately equal 0.55 and 0.64, respectively. We have found the mixtures S1 and S2 to yield similar values for the RLP and RCP states; the former occurring during the gravity compaction (GC) phase and the latter arising at the end of the uniaxial compaction (UC) phase, as shown in Fig. 1. The linear increase in the packing fraction after time $t \approx 0.8$ s occurs during the UC phase. The particles are found to settle within a decreasing interval of time, from the commencement of the simulation, with increasing surface friction, for both samples. This is an expected result (Silbert, Ertas, Grest, Halsey & Levine 2002), as the surface friction will tend to oppose the relative velocity at the contact surface. In fact, the packing fraction for the samples during the GC and the UC phases are consistently lower with increasing friction. The results indicate that for a given value of the surface friction, the packing fraction during both phases of the simulation is higher for sample S2 than sample S1. A likely explanation of this finding is as follows: a sample with a larger fraction of relatively 'softer' particles will tend to pack more efficiently due to the increased deformability of the particles. Our computations of the distribution of contacts, as shown in Fig. 2, suggests a similar behavior. The contact distributions for the various cases after the GC phase is not too distinguishable; however, after the UC phase, the contact distribution for sample S2 ($\mu_k = \mu_{stat} = 0.1$) has a significant shift towards a higher number of average contacts as opposed to that for sample S1 ($\mu_k = \mu_{stat} = 0.1$). For samples S1 and S2 with $\mu_k = \mu_{stat} = 0.2$, the difference in the contact distribution is less distinguishable. A point to note is that after the GC phase, about 10 % of the spheres have three or less contacts; this fraction decreases with friction and increasing fraction of 'softer' particles. This observation arises due to the particles located on the top of the pile, or continuing to settle under grav-

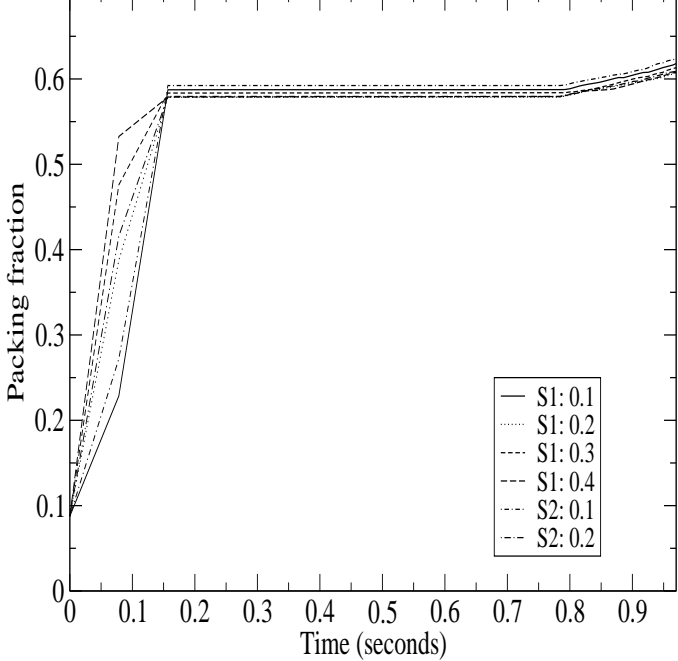


Figure 1. The evolution of the packing fraction during the GC and the UC phases of the simulation. The compaction phase begins from time $t \approx 0.8$ s.

ity. After the UC phase, this fraction of particles decreases significantly. Another quantitative measure of the packing structure is the radial distribution function (RDF) which will indicate the degree of close or ordered packing in the system. Fig. 3 shows the RDF for the different instances of the various numerical experiments after completion of the GC and the UC phases. The first amplitude represents the nearest neighbor contacts as it occurs at $r \approx 1$. The amplitudes at $r \approx 1.75$ and 2 in-

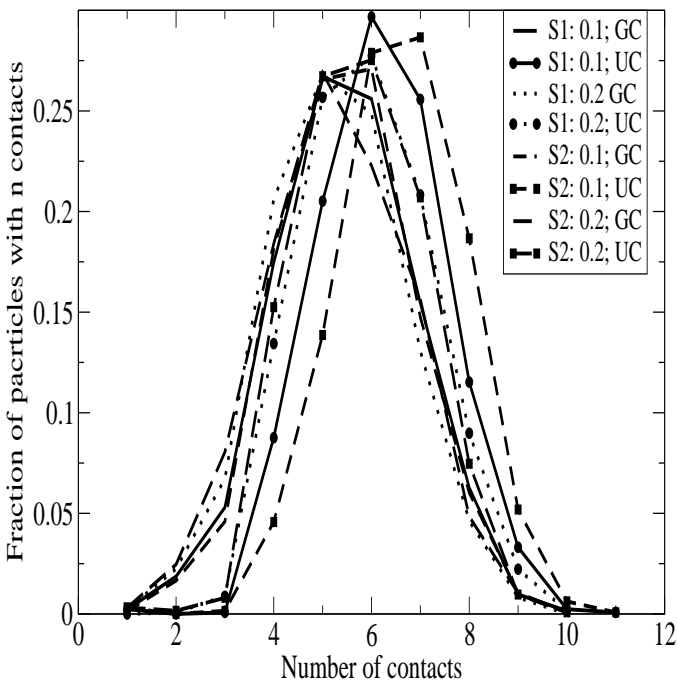


Figure 2. The fraction of particles with a given number of contacts after the GC and the UC phases of the simulation.

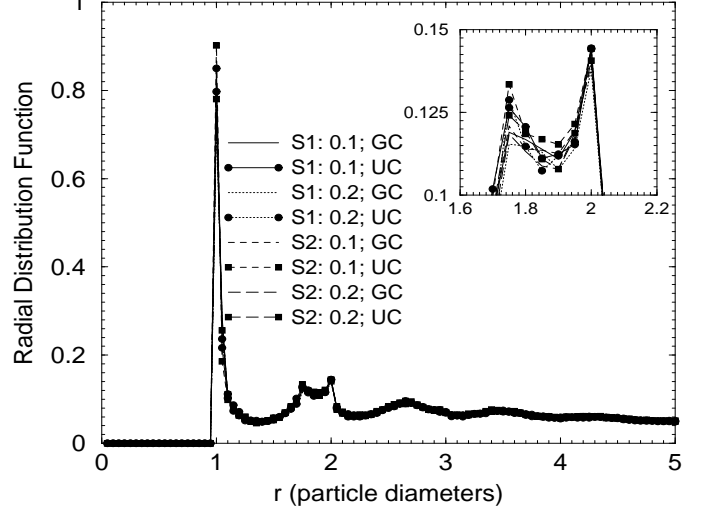


Figure 3. Radial distribution function after the GC phase (solid line) and the UC phase (dotted lines) for the various samples. The inset focuses on the second and third peaks of the RDF.

coupled with the decrease in the difference between the amplitudes indicates that close packing is occurring (Clarke & Jonsson 1993). This trend in the behavior is particularly evident for sample S2 ($\mu_k = \mu_{stat} = 0.1$). The inset of Fig. 3 magnifies the RDF amplitudes occurring at $r \approx 1.75$ and 2. The distribution of the angles the contact vector (the vector connecting the centers of mass of the two particles in contact) makes with the vertical can be used to provide insight into the packing structure. The distribution shows the particle contacts to reorient themselves in response to the applied strain. There is, however, very little difference between the results for the two samples.

Understanding the distribution of the contact forces throughout the contact network of the particle agglomerate provides a valuable insight into how the load is supported through the packing. The question we ask is whether there is any difference in the functional form and in the evolution of the contact force distributions with variation in the individual material components of the mixture. In this paper, we present results exploring the distribution of the normal contact forces before and after the UC phase, for the two mixtures S1 and S2. Fig. 4 shows the normal contact force distributions $P(F_n)$ before and after the UC phase, for the samples S1 and S2. Each normal contact force F_n has been normalized by the average normal contact force ($\langle F_n \rangle$ where $f_n = F_n / \langle F_n \rangle$) for each set of results. Before the commencement of the UC phase, the particles are on the average in a mechanically stable spatial configuration by the stabilization of the packing fraction, as demonstrated in Fig. 1, and the coordination number. Before the UC phase, we find the distribution of the strong forces ($f_n > 1$) to follow an exponential functional form ($P(f_n) \propto \exp(-\beta f_n)$); implying that most of the strong forces are supported

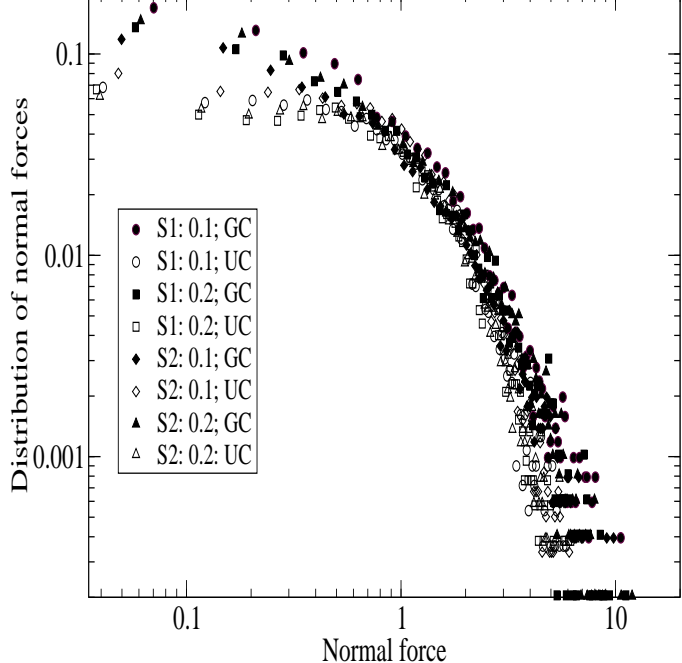


Figure 4. The normal contact force distribution $P(f_n)$ ($f_n = F_n / \langle F_n \rangle$) for the samples S1 and S2, before and after the UC phase.

by a small number of contacts. After the UC phase, we find the contact force distributions to gradually evolve to the Gaussian functional force ($P(f_n) \propto \exp(-\alpha f_n^2)$), indicating a more even distribution of the load throughout the contact network (Liu, Nagel, Schecter, Majumdar, Narayan & Witten 1995)-(Thornton & Anthony 1998). For the weak contact forces ($f_n < 1$), we find our results to agree with the existing studies which have shown the distribution of the weak contact forces to adhere to a power law functional form. However, our results do not indicate any difference in the functional forms or the evolution of the contact force distributions for the different samples. There could be a few explanations for this observation: the difference in the material properties of the excipients studied is not too significant, and the UC phase lasts for a very short duration. We have obtained similar results from our computations of the tangential contact force distributions. Currently we are looking into the effect of introducing particle size dispersity in our excipient mixtures on the response to an external strain.

5 DISCUSSIONS

Our studies on the geometric characteristics and the material response of the particle packings of excipient mixtures have not yielded any significant differences between the mixtures. A possible explanation for these findings may be due to the small difference in the Young's modulus and Poisson ratio values for the three materials, or the very short duration of the UC phase. In our future work, we will further address these issues. As mentioned earlier, we have also been exploring the effect of

size dispersity on the response to externally applied strain by these mixtures. These results will be presented elsewhere.

We would like to acknowledge Pfizer for providing funding support.

REFERENCES

- Åström, J.A., Herrmann, H.J. and Timonen, J. 2000, Granular packings and faults, *Phys. Rev. Lett.* 84 638.
- Pharmaceutical Powder Compaction Technology, Marcel Dekker Inc., New York 1996, Ed. Goran Alderborn and Christer Nyström.
- Clarke, A.S. and Jonsson, H. 1993, Structural changes accompanying densification of random hard-sphere packings, *Phys. Rev. E* 47 3975.
- Cundall, P.A. and Strack, O.D.L., A discrete numerical model for granular assemblies, *Géotechnique* 29 47.
- Dutt, M., Hancock, B., Bentham, C. and Elliott, J. 2005, An implementation of granular dynamics for simulating frictional elastic particles based on the DL_POLY code, *Comp. Phys. Comm.* 166 26.
- Hidalgo, R.C., Grosse, C.U., Kun, F., Reinhardt, H.W. and Herrmann, H.J. 2002, Evolution of percolating force chains in compressed granular media, *Phys. Rev. Lett.* 89 205501.
- Jaeger, H.M., Nagel, S.R. Nagel, and Behringer, R.P. 1996, Granular solids, liquids and gases, *Rev. Mod. Phys.* 68 1259.
- Liu, C.-h., Nagel, S.R., Schecter, D.A., Majumdar, S.N., Narayan, O. and Witten, T.A. 1995, Force fluctuations in bead packs, *Science* 269 513.
- Makse, H.A., Johnson, D.L. and Schwartz, L.M. 1999, Packing of compressible granular materials, *Phys. Rev. Lett.* 83 5070.
- Makse, H.A., Gland, N., Johnson, D.L. and Schwartz, L.M. 2000, Why effective medium theory fails in granular materials, *Phys. Rev. Lett.* 84 4160.
- Schäfer, J., Dippel, S. and Wolf, D.E. 1996, Force schemes in simulations of granular materials, *J. Phys. I France* 6 5.
- Silbert, L.E., Ertas, D.E., Grest, G.S., Halsey, T.C. and Levine, D. 2002, Geometry of frictionless and frictional sphere packings, *Phys. Rev. E* 65 031304.
- Silbert, L.E., Ertas, D.E., Grest, G.S., Halsey, T.C. and Levine, D. 2002, Analogies between granular jamming and the liquid-glass transition, *Phys. Rev. E* 65 051307.
- Silbert, L.E., Grest, G.S. and Landry, J.W. 2002, Statistics of the contact network in frictional and frictionless granular packing, *Phys. Rev. E* 66 061303.
- Thornton, C. and Anthony, S.J. 1998, Quasi-static deformation of particulate media, *Phil. Trans. R. Soc. Lond. A* 356 2763.